The Astrophysical Journal, 578:385–390, 2002 October 10

POSSIBLE EVIDENCE FOR PULSED X-RAY EMISSION FROM THE OUTER GAP IN PSR B1937+21

H. G. Wang, R. X. Xu, and G. J. Qiao
Department of Astronomy, Peking University, 5 Haidian Lu, Beijing 100871, China
Received 2002 March 23; accepted 2002 June 13

ABSTRACT

The fastest millisecond pulsar PSR B1937+21 presents an interpulse separated from the main pulse by nearly 180° at radio frequencies. Recently, the *ASCA* observations detected pulsed X-ray emission from this pulsar. Only a single narrow X-ray pulse is observed, which is coincident with the radio interpulse in phase. We investigate the possible origin of the pulsed X-rays from the polar cap (PC) accelerators or the outer gap (OG) accelerators in the frame of a PC model and an OG model, respectively, by assuming a dipolar magnetic field structure and the same radio emission pattern from its poles for the pulsar. The OG model can naturally explain the main observational facts. For the PC model, the coincidence between the X-ray pulse and the radio interpulse cannot be reproduced in the assumed case. However, when considering possible deviation from our assumption, the PC model may still be valid for this pulsar in some cases.

Subject headings: pulsars: individual (PSR B1937+21) — radiation mechanisms: nonthermal — X-rays: stars

1. INTRODUCTION

Even more than 30 years after the discovery of high-energy pulsars, the theoretical reproduction of X-ray and γ-ray emission from such pulsars is still a matter of debate. It is commonly agreed that there are two scenarios on modeling X-ray and γ-ray creation: the outer gap (OG) model (e.g., Cheng, Ho, & Ruderman 1986a, 1986b; Romani 1996; Cheng & Zhang 1999; Hirotani & Shibata 2001) and the polar cap (PC) model (e.g., Harding 1981; Sturner & Dermer 1994; Daugherty & Harding 1996; Luo, Shibata, & Melrose 2000; Zhang & Harding 2000). The fundamental difference between these two types of models is the location of the regions where particles are accelerated to relativistic energies and emit high-energy photons. The early PC model (Harding 1981) assumed that the emission is produced just above the PC surface. In the present versions of the PC model (e.g., Daugherty & Harding 1996; Harding & Muslimov 1998), it is proposed that the particle acceleration region may extend from the PC surface to several stellar radii above because of free charge flow and inertial frame dragging, so that wide, double-peaked X-ray and γ-ray light curves can be reproduced, given that the inclination angle is not large. In contrast, the OG model (Cheng et al. 1986a, hereafter CHR) presumed that the gaps can exist in the outer magnetosphere between the null charge surface and the light cylinder. Later, the CHR model was developed to the single OG models (e.g., Chiang & Romani 1994; Romani & Yadigaroglu 1995; Cheng, Ruderman, & Zhang 2000), which claimed that the three-dimensional extent of OGs are constrained by the pair cascade processes and that a single OG can produce wide, double-peaked high-energy light curves. Whereas theoretical considerations of more detailed physical processes for particle acceleration and photon emission are necessary, it is urgent and interesting to find new observational evidence for these models.

PSR B1937+21, with the period of 1.56 ms, is the fastest millisecond pulsar (MSP) known. At radio bands, it exhibits an interpulse emission that is roughly equal to the main pulse in intensity and separated from it by a phase of about 180°. Recently, the *ASCA* observations detected pulsed X-ray emission from this pulsar (Takahashi et al. 2001). Only one nonthermal narrow pulse was observed, which is coincident with the radio interpulse in phase, within the timing errors. The pulse width is about 100 ± 61 μs ($23° \pm 14°$). Besides the narrow pulse, the light curve reveals two additional wide Gaussian-shaped bulges above the background level, with each phase interval being about 0.5 rotation periods and each peak intensity $\sim\frac{1}{4}$ of the nonthermal pulse peak.

Where does the X-ray emission of the fastest MSP come from, the PC or the OG? It has not been as extensively studied as the other high-energy pulsars such as the Crab pulsar and Vela. The previous work was done by Luo et al. (2000), in which the PC model was modified for MSPs. They applied the theory to PSR B1937+21 and suggested that the X-ray emission probably originates from the location of one stellar radius above the PC.

In this paper efforts on modeling the observational data at radio and X-ray bands are made for both the PC and OG models. The inclination angle between the rotation and magnetic axes is constrained in § 2, which is necessary for the modeling. The modeling is carried out in § 3. Conclusions and discussions are placed in § 4.

2. THE INCLINATION ANGLE

The inclination angle (α) between the rotation and magnetic axes is a necessary parameter for both the PC and OG models to give various high-energy emission beams. Unfortunately, there is no agreement on the value of the inclination angle of PSR B1937+21. In this section we reinvestigate the value of α under the double-pole model, viz., the radio interpulse and main pulse are considered to be from the opposite magnetic poles of a dipolar field, and the result is used in the calculation in § 3.

We assume that the radio emission beams from double poles are axisymmetric around the magnetic axis and have the same radius, namely, $\rho_1 = \rho_2$. According to the geometry model (Gil, Gronkowski, & Rudnicki 1984; Lyne &

Manchester 1988) one has

$$\sin^2\frac{\rho_1}{2}=\sin^2\frac{W_1}{4}\sin\alpha_1\sin(\alpha_1+\beta_1)+\sin^2\frac{\beta_1}{2}\ , \quad (1)$$

$$\sin^2\frac{\rho_2}{2}=\sin^2\frac{W_2}{4}\sin\alpha_2\sin(\alpha_2+\beta_2)+\sin^2\frac{\beta_2}{2}\ , \quad (2)$$

where β is the impact angle between the line of sight (LOS) and the magnetic axis, W is the pulse width of the average profile, and the subscripts "1" and "2" denote the main pulse and the interpulse, respectively. There are two simple geometrical relations between the inclination angles and the impact angles, namely, $\alpha_2=\pi-\alpha_1$, and $\beta_2=\alpha_1+\beta_1-\alpha_2$.

From the above relations β_1 can be derived as

$$\beta_1=\tan^{-1}\left[\frac{A-\tan^2\alpha_1}{(A+1)\tan\alpha_1}\right], \quad (3)$$

where

$$A=\frac{1}{\sin^2(W_1/4)-\sin^2(W_2/4)}\ . \quad (4)$$

In the following we neglect the subscript "1," so that all the α, β, and ρ below refer to the main pulse except for the special declaration.

To figure out the value of A, the profile at 1.5 GHz is chosen (downloaded from the European Pulsar Network)-for its high time resolution and low-dispersion smearing (Kramer et al. 1998). The pulse widths are measured at the level of 10% of their peak intensities, which are $19\overset{\circ}{.}4\pm0\overset{\circ}{.}4$ and $17\overset{\circ}{.}8\pm0\overset{\circ}{.}4$ for the main pulse and the interpulse, respectively. So that $\beta(\alpha)$ and $\rho(\alpha)$ can be calculated, as shown by the solid curve and the curve marked with open circles, respectively, in Figure 1. The $\beta(\alpha)$ curve approximates a linear function of $\alpha+\beta\approx90^\circ$, when $\alpha\lesssim85^\circ$, which is determined by the fact that the main pulse and interpulse are both narrow and differ only a little in pulse width.

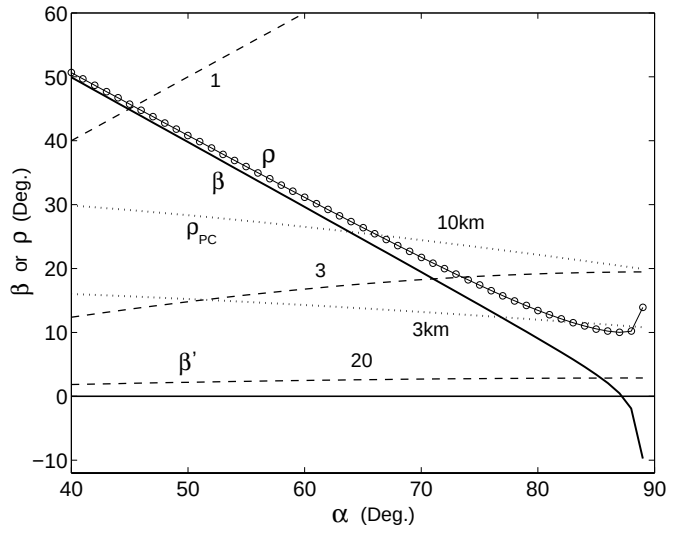

FIG. 1.—Plot of β and ρ as functions of inclination angle α. The curves of $\beta(\alpha)$ and $\rho(\alpha)$ are derived from the observational pulse widths. The dashed curves are $\beta'(\alpha)$ derived from eq. (5), given $(d\psi/d\phi)_{\max}=1,3$, and 20, respectively. The dotted curves are the opening angle of the polar cap ($\rho_{\rm PC}$), given $R=3$ and 10 km.

For a dipolar field, the shape of the polar cap is found to change from a circle (for $\alpha=0^\circ$) to an ellipse, of which the longitudinal radius is about 1.6 times the latitudinal radius (for $\alpha=90^\circ$; Cheng et al. 2000). Since the deviation from circular shape is not essentially significant, we simply regard the polar cap as a circle in this section so that the opening angle (between the magnetic axis and the tangent of the magnetic field line) of the polar cap $\rho_{\rm PC}$ can be determined by the last open field line on the plane containing the rotation and magnetic axes (Ω-μ plane). The radius $\rho_{\rm PC}$ is a function of the stellar radius R and the inclination angle α, as shown by the dashed curves in Figure 1 for $R=3$ and 10 km.

We further assume that if the boundary of the radio beam is defined by the last open field lines, then the beam radius should be greater than $\rho_{\rm PC}$. According to this criteria, the inclination angle is constrained to be $\alpha\lesssim63^\circ$ for $R=10$ km and $\alpha\lesssim77^\circ$ for $R=3$ km. As the radii of neutron stars (NSs) are currently believed to be about 10 km, we accept that $\alpha\lesssim63^\circ$.

Can we determine the exact value of α? It is certain if the maximum rate of position angle $(d\psi/d\phi)_{\max}$ is exactly known, where ψ is the position angle and ϕ is the pulse longitude. The maximum rate presents the second relationship between α and β, which reads

$$\left(\frac{d\psi}{d\phi}\right)_{\max}=\frac{\sin\alpha}{\sin\beta}\ . \quad (5)$$

Combined with equations (3) and (5), α and β can be solved for a given $(d\psi/d\phi)_{\max}$.

Although recent polarization observations present flat position angle sweeps (Thorsett & Stinebring 1990; Stairs, Thorsett, & Camilo 1999), it cannot be asserted that the real value of $(d\psi/d\phi)_{\max}$ is small, because observations may give a less steep position angle gradient because of the smearing of finite sampling time, the frequency dispersion in pulse arrival time (Liu & Wu 1999), and the interstellar scattering (Gil 1985a). The $\beta'(\alpha)$ curves derived from equation (5) for $(d\psi/d\phi)_{\max}=1,3$, and 20, respectively, are presented by the dotted curves in Figure 1. The intersection of $\beta'(\alpha)$ and $\beta(\alpha)$ shows that a larger $(d\psi/d\phi)_{\max}$ results in a larger α and smaller β, which means that the LOS sweeps across the radio beam closer to the beam center.

One may find that when the real value of $(d\psi/d\phi)_{\max}$ is large enough, α would exceed 63° [for example, taking $(d\psi/d\phi)_{\max}=3$, as proposed by Gil 1985a, α is 71°] and hence contradicts $\alpha\lesssim63^\circ$. However, if the radius is smaller, for example, $R=3$ km, this inconsistency would cancel. In fact, Xu, Xu, & Wu (2001) suggested that PSR B1937+21 is probably a strange star (SS) with low mass and small radius. The detailed discussion is in § 4.

The range of α presented above is different from the conventional consideration in double-pole model that α should be close to 90° (Stairs et al. 1999). Alternatively, there is another kind of so-called single-pole model to interpret the interpulse, which suggests that the interpulse emission comes from the same pole as the main pulse. In the single-pole model proposed by Gil (1985a) for PSR B1937+21, α only needs to be 20°. The single-pole model predicts that the separation between the main pulse and interpulse may be close to 180° and is frequency independent (Gil 1983, 1985b), which is coincident with the observation of PSR B1937+21 (Hankins & Fowler 1986). However, observa-

tions with high time resolution (e.g., Kramer et al. 1998; Stairs et al. 1999) failed to find the emission components between the main pulse and interpulse, which were reported by Stinebring et al. (1984) and were suggested to be a strong support to the single-pole model (Gil 1985a). Therefore, in this paper the radio emission is considered to come from double poles. More confirmative estimations of $(d\psi/d\phi)_{\max}$ are expected to determine α and β.

3. THE ORIGIN OF NONTHERMAL X-RAY EMISSION FROM PSR B1937+21

In this section we calculate the X-ray beams in the frames of both the PC and OG models to find out whether they are able to reproduce the observational facts. The following facts are used here:

1. At 1.4 GHz the separation between the peaks of the interpulse and main pulse is 174° (measured from the profile presented by Takahashi et al. 2001).
2. At 1.5 GHz (EPN data) the 10% widths of the main pulse and interpulse are 19°.4 and 17°.7, respectively.
3. The nonthermal X-ray pulse is nearly coincident with the interpulse; the X-ray pulse width is about 23° (Takahashi et al. 2001).

3.1. *Origin from the PC Accelerators?*

Luo et al. (2000) discussed the viability of PC models for high-energy emission from MSPs. They found that the maximum Lorenz factor of particles is limited by curvature radiation and is not sensitive to the specific acceleration model, but the height where the Lorenz factor achieves the maximum is model dependent, which may be between 0.01 R (for the inner vacuum gap) and above 0.1 R (for the space-charge limited gap) from the PC surface for pulsar period $P = 2$ ms and a surface magnetic field of $B_s = 7.5 \times 10^8$ G. Assuming a space-charge limited flow, the pair cascades can occur at the typical distance (to the star center) of $r \simeq (1.5\text{–}2.5)\ R$, and high-energy emission is radiated from this region. With respect to $P = 1.56$ ms and $B_s = 4.1 \times 10^8$ G for PSR B1937+21, their analysis applies to this pulsar.

Since the radio emission is also radiated from the region near the PC, homocentric radio and X-ray beams are produced (Fig. 2*a*). Quantitatively, we assume the radio emission arises from the PC up to the distance $r = 2.5\ R$, the X-rays may arise from the PC to (*a*) a relatively higher distance, e.g., $r = 3\ R$, or (*b*) a lower distance, e.g., $r = 2\ R$. For simplicity we assume the emission regions are bounded by the last open field lines. In case *a* the X-ray beams are wider than the radio beams, therefore, when the line of sight sweeps across both radio beams (to reproduce the main pulse and the interpulse) it would sweep across both X-ray beams also, and hence give a double X-ray pulse, which is inconsistent with the observation. In case *b* the X-ray beams are narrower than the radio beams, and then, for a proper viewing angle (between LOS and the rotation axis), only one X-ray beam could be observed. In this case, could fact 3 be explained as well? We analyze this issue by using the figure of the (phase-viewing angle) plane on which the emission beams are projected.

In Figure 3 the horizon axis is pulse phase, and the vertical axis is the viewing angle ζ ($\zeta = \alpha + \beta$). The dotted curves represent the boundaries of the X-ray beams, the solid curves are the boundaries of the radio beams, and the PCs are shown by the dashed curves. Retardation (due to distinct emission heights) and aberration effects (due to emission sources corotating with the pulsar) have been taken

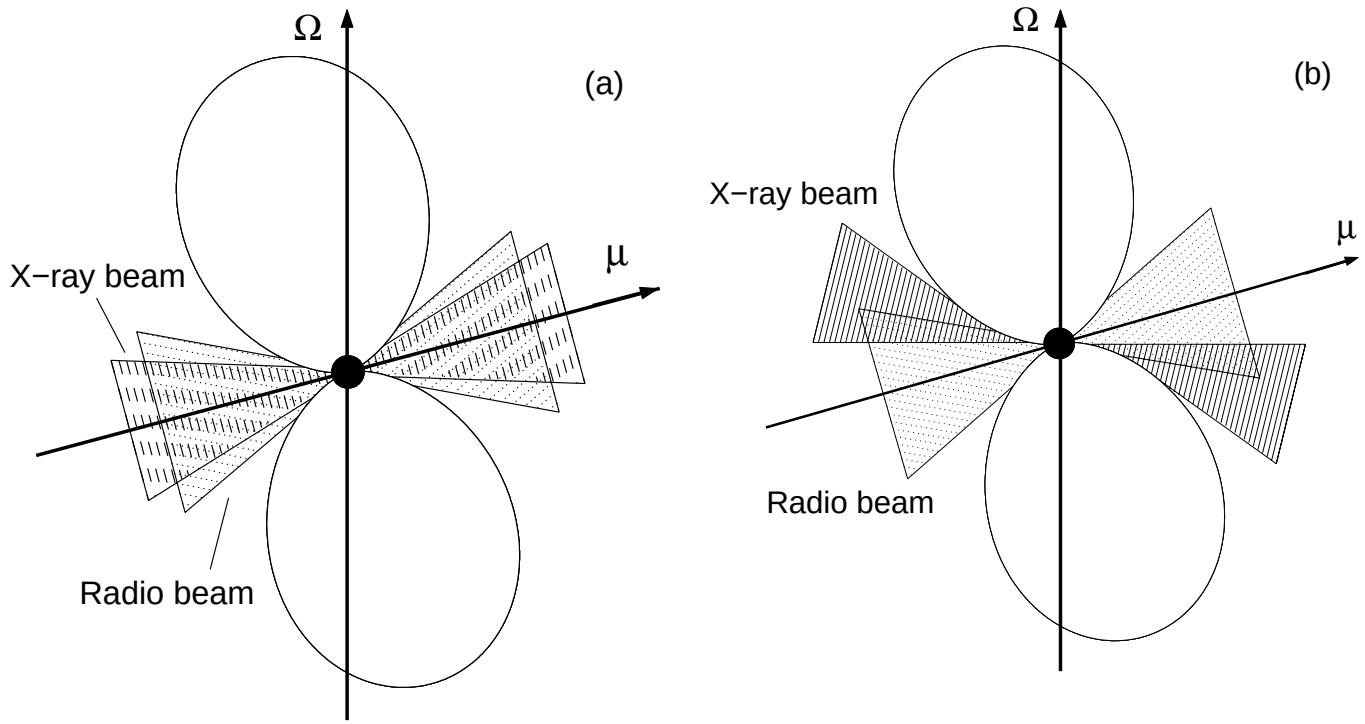

FIG. 2.—(*a*) Scheme for the X-ray beams in the frame of the PC model. (*b*) Scheme for the X-ray beams produced by the OG model. Radio beams are also plotted.

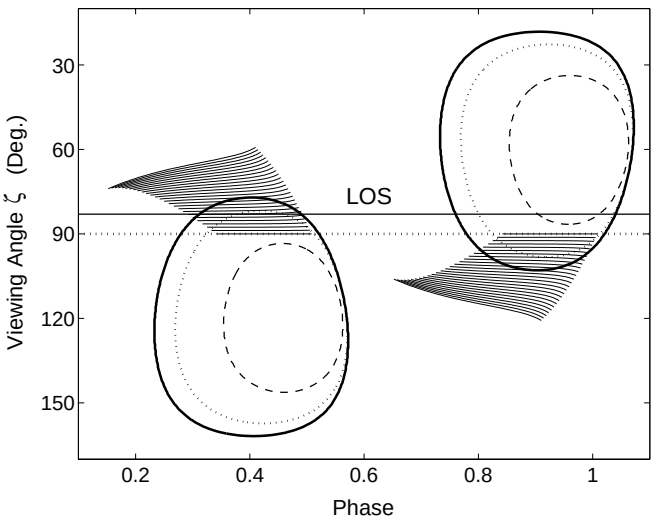

FIG. 3.—Emission beams projected onto the (phase-viewing angle) plane for $\alpha = 60°$. The solid curves are the boundaries of radio beams, the dotted curves are the boundaries of X-ray beams from the extended acceleration zones above the PCs suggested by the PC model, the shaded areas are the X-ray beams from the outer gaps, and the dashed curves represent the PCs (see text and the first line of Table 1 for the related parameters).

into account, both of which make the lower beam move toward the trailing edge of the higher beam. To obtain the figure, a moderate inclination angle is taken, $\alpha = 60°$. Although there is $\alpha \lesssim 63°$, as discussed in § 2, the angle should not be too small, or it would give excessively wide radio beams (Fig. 1), which must be emitted from unbelievably high distances near the light cylinder.

According to Figure 3, when $\zeta \simeq 80°$, the X-ray peak is coincident with the radio pulse centered on phase about 0.9; when $\zeta \simeq 100°$, it is coincident with the radio pulse on phase about 0.4. However in both cases, the radio pulse associated with the X-ray pulse is the main pulse that is wider and more intense than the other one.

However, we should point out that the above analysis is based on a simple assumption that the radio (X-ray) beams from both poles have the same width, and the emission pattern in the beams is symmetrical about the magnetic axis. Since the magnetosphere structure of pulsars and the detailed radio emission process are still not exactly known, possibly significant deviation from the assumption cannot be ruled out, and the validity of the PC model needs to be considered further. We discuss such a possibility in § 4.

3.2. *Origin from the OG Accelerators*

In the original OG model CHR suggested that a global current flow through the magnetosphere can result in large regions of OGs between the null charge surface and the light cylinder along the last open field lines. Within the OGs particles with one kind of charge are accelerated outward from the star and give an outward emission beam, while those with the opposite charge are accelerated toward the star and give an inward beam. The high-energy photons were proposed to be emitted from two OGs associated with the two poles so that the double-peaked γ-ray pulse profile can be reproduced, of which one peak corresponds to the outward beam from one OG and the other peak corresponds to the inward beam from the opposite OG. CHR assumed that the OGs are active only near the Ω-μ plane. However, this assumption is merely valid for large inclination angles.

The currently prevalent OG models are the single OG models (e.g., Chiang & Romani 1992, 1994; Cheng et al. 2000). Generally the inward emission is not important in these models for the reason that the inward high-energy photons cannot pass freely through the inner magnetosphere due to magnetic pair production. The outward emission from the OG associated with a single pole can produce a broad, irregularly shaped emission beam that is particularly dense near the edge. The OG regions can be supported along all the last open field lines, but the three-dimensional scales of OGs are limited by the pair production processes.

In the latest version of this type of model (Cheng et al. 2000), the fraction size ($f \equiv h/R_{\rm L}$) of the gap is $f \simeq 5.5 P^{26/21} B_{12}^{-4/7} \xi^{-1/7}$, which can be estimated by the threshold of γ-γ pair production, $E_{\rm X}(f) E_{\gamma}(f) \geq (m_{\rm e}c^2)^2$, where h is the mean vertical extension perpendicular to the magnetic field, R_L is the radius of the light cylinder, $\xi = \Delta\phi/2\pi$, $\Delta\phi$ is the transverse extension of the gap, $E_{\rm X}$ is the energy of the X-ray photons emitted from hot PCs, and E_{γ} is the characteristic photon energy emitted by the relativistic particles. The radial scale of pair production is limited to a range between $r_{\rm in}$ and $r_{\rm lim} \sim 6 r_{\rm in}(\xi = 0)$, where $r_{\rm in}$ (the subscript "in" means the inner boundary of the OG) is the distance of null charge surface and $\xi = 0$ corresponds to the Ω-μ plane.

In the following our modeling is in the frame of a single OG model. Only the outward emission beams from two OGs are considered, as illustrated by Figure 2*b*. For PSR B1937+21, we have a thin OG with $f = 0.16\xi^{-1/7}$, so that the X-rays can be simply regarded as being radiated from the last open field lines, unless ξ is too small. The radial scale $r_{\rm lim}/r_{\rm in}$ and the transverse scale ξ are free parameters in calculating the X-ray beams.

First, we consider a general situation of the OG scenario to test if the observational facts can hopefully be reproduced. From Figure 2*b* one can see that provided the observer's viewing angle is not just 90°, e.g., $\zeta = 83°$, the LOS can sweep across both of the radio beams and only one X-ray beam. By assuming a group of reasonable values of parameters (see the first line of Table 1), namely, the inclination angle, the stellar radius, the distance of radio emission, and the radial and transverse extensions of the OGs, the X-ray beams are calculated, which are demonstrated by the shaded areas in Figure 3. Retardation and aberration effects are also included. It shows clearly that the X-ray pulse could be associated with the radio interpulse (which has a smaller width than the other one), and the narrow X-ray pulse width may be obtained if a proper extension of the OG is assumed.

Then we model the observational data. The parameters listed in the second line of Table 1 are found to be able to

TABLE 1

PARAMETERS FOR CALCULATING THE RADIO AND X-RAY BEAMS/PROFILES

No.	α (deg)	ζ (deg)	R (km)	$r^{\rm a}$ (R)	$r_{\rm in}(0)^{\rm b}$ (R)	$r_{\rm lim}/r_{\rm in}$	$\Delta\phi$ (deg)
1.....	60	...	10	2.5	1.3	3.5	100
2.....	55	89.5	10	1.7	1.5	2.0	40
3.....	75	89.5	2	2.9	2.1	2.5	66

[a] The distance of radio emission, in units of stellar radii R.
[b] The distance of the null charge surface on the Ω-μ plane.

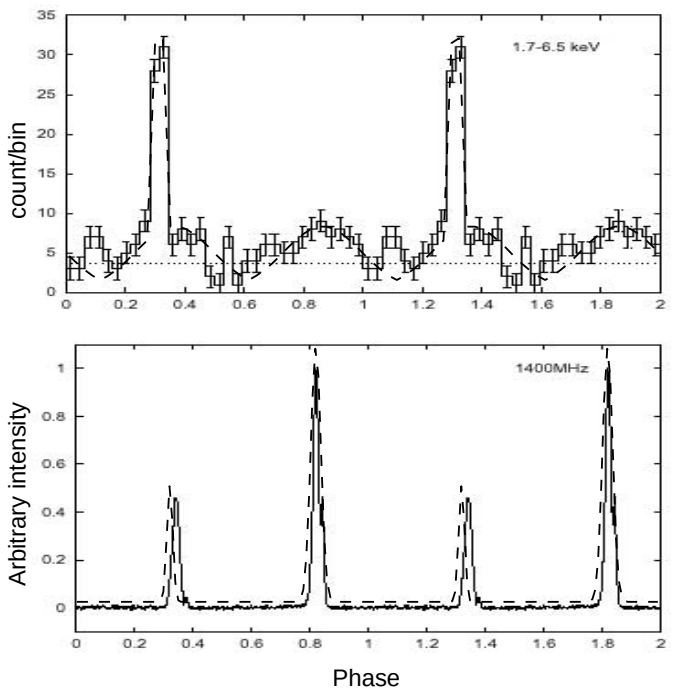

FIG. 4.—Theoretical X-ray and radio profiles (*dashed curves*) together with the observational profiles (Takahashi et al. 2001). The parameters in the second line of Table 1 are used to obtain the theoretical profiles.

reproduce the narrow X-ray pulse width, the radio pulse widths, and the coincidence between the X-ray pulse and the radio interpulse, which are in good agreement with the observational data. In order to simulate the observational profiles, we simply assume that the X-ray and radio pulses are Gaussian shapes and assume additionally wide, weak, hot X-ray emission from both of the PCs. The theoretical profiles are plotted in Figure 4, together with the observational profiles for comparison.

It should be pointed out that modeling the X-ray pulse width is not sensitive to the value of $r_{\rm lim}/r_{\rm in}$ but to ξ, thereby the range of $r_{\rm lim}/r_{\rm in}$ is relaxed and a reasonable value is chosen. Other groups of values are also tried. It is found that for the moderate inclination angles $40^\circ \lesssim \alpha \lesssim 63^\circ$, the observational data can be reproduced with a proper choice of the gap size ($\xi = 40^\circ$ in Table 1 is approximately the maximum transverse scale). Therefore, our calculation suggests that the nonthermal X-rays of PSR B1937+21 may be emitted from the OGs.

4. CONCLUSIONS AND DISCUSSIONS

The discovery of pulsed X-ray emission from the MSP PSR B1937+21 and the phase alignment between the X-ray pulse and the radio interpulse provide valuable information on the emission mechanism. In this paper we investigate the possible origin of the X-rays from both the PC and OG accelerators. In the frame of the prevailing OG model (e.g., Cheng et al. 2000), the X-rays from outer gap accelerators could account for the main observational facts by assuming a proper size of the OGs for an oblique rotator. In the frame of the PC model, by assuming symmetric geometry for radio and X-ray emission, the X-rays from polar cap accelerators would produce an X-ray peak aligned with the main radio pulse in phase, which contradicts the observation.

Some more discussions for both the OG and PC models are presented as follows. First we refer to the OG model.

There is a slight inconsistency as shown in Figure 4, i.e., in the OG model, the calculated separation between the interpulse and main pulse is 180°, 6° greater than the observational value. This may be due to the retardation effect. The phase shift for different heights can be roughly estimated as $\Delta s = \Delta r/(Pc)$. A difference of $\Delta r = 0.8\,R$ is enough to produce the phase shift of 6°.

A moderate inclination angle of 55° is used in the modeling. But α could be larger if the real gradient of the position angle is steeper than the present observations as suggested in § 2. Could the OG model be still valid for large values of α?

As shown in Figure 1, when $(d\psi/d\phi)_{\rm max} \gtrsim 4$, it would result in a puzzling problem in that the derived radio beam radius is considerably smaller than the PC radius, if $R = 10$ km and a magnetic dipole are assumed. A much smaller stellar radius could cancel the problem, but this requires an SS scenario, because the smallest radius of NSs is generally believed to be ~9 km, while SSs can have much smaller radii due to their different equations of state. In fact, according to the observational limits on the radius and mass derived from the pulse width and $(d\psi/d\phi)_{\rm max}$, Xu et al. (2001) suggested that PSR B1937+21 is probably a strange star with very low mass, small radius, and weak magnetic moment. If PSR B1937+21 is an SS with small radius, for example, $R = 2$ km, a group of parameters is found out to be able to model the observational data by OG model, which is listed in the third line in Table 1.

Then we turn to the PC model. When the emission geometry is not symmetrical, the PC model could be able to explain the observation as well. The possible asymmetry is discussed for the radio and the X-ray emission, respectively.

1. It has been assumed that the radio emission pattern from the two poles is the same in our modeling; the different behaviors of the main pulse and the interpulse are thus geometrical origin. However, their difference may be caused intrinsically since the mechanism for the radio emission is still poorly understood. For example, a possible reason may be that the pulsar has a nondipolar magnetic field, thus the distribution of emission intensity in the radio beams may be different from each other, which could lead to the case that for one beam only part of it is observed, while for the other a larger part or the whole is observed.

2. When PSR B1937+21 is an NS or an SS with crust and its inclination angle is near 90°, the X-ray emission pattern may be significantly asymmetric about the magnetic axis. In this case, the space charge is negative on the side toward the rotation axis (where $\mathbf{\Omega} \cdot \boldsymbol{B} > 0$, hereafter side I) and positive on the side away from the axis (where $\mathbf{\Omega} \cdot \boldsymbol{B} < 0$, hereafter side II). On side II the ions can be pulled away from the surface by strong electric field if the binding energy is small enough. Therefore, the half-beam from side II could be much less luminous than that from side I due to the much smaller Lorentz factors of the ions, and thus may be too weak to be observed. Notice that, if side I is above the equator on one pole, it should be below the equator on the other pole. Therefore, only single X-ray peak is observed which may coincide with the radio interpulse.

In recent years, it is suggested that pulsars may be bare strange stars (BSSs; e.g., Xu 2002 and references therein). If

PSR B1937+21 is also a BSS, the positive charge on side II is carried by positrons but not ions, then the emission pattern on both sides should be the same, and each beam may be symmetric around the magnetic axis. In this case, when symmetrical geometry is assumed for the radio emission, the PC model could not account for the observational facts, otherwise, the PC model may still be valid.

In general, further research on the pulsar's magnetosphere structure and emission mechanisms will be helpful in understanding the origin of its X-rays for PSR B1937+21. We are expecting that future polarization observations could provide a more confirmative value of $(d\psi/d\phi)_{\max}$, which is meaningful not only for constraining whether this pulsar is an NS or an SS but also for a better understanding of its X-ray emission.

We are grateful to J. A. Gil and B. Zhang for their helpful comments and discussions. The valuable suggestions from an anonymous referee are also sincerely acknowledged. This work is supported by National Nature Science Foundation of China (10173002) and by the Special Funds for Major State Basic Research Projects of China.

REFERENCES

Cheng, K. S., Ho, C., & Ruderman, M. A. 1986a, ApJ, 300, 500
———. 1986b, ApJ, 300, 522
Cheng, K. S., Ruderman, M. A., & Zhang, L. 2000, ApJ, 537, 964
Cheng, K.S., & Zhang, L. 1999, ApJ, 515, 337
Chiang, J., & Romani, R. W. 1992, ApJ, 400, 629
———. 1994, ApJ, 436, 754
Daugherty, J. K., & Harding, A. K. 1996, ApJ, 458, 278
Gil, J. 1983, A&A, 127, 267
———. 1985a, A&A, 143, 443
———. 1985b, ApJ, 299, 154
Gil, J., Gronkowski, P., & Rudnicki, W. 1984, A&A, 132, 312
Hankins, T. H., & Fowler, L. A. 1986, ApJ, 304, 256
Harding, A. K. 1981, ApJ, 245, 267
Harding, A. K., & Muslimov, A. G. 1998, ApJ, 508, 328
Hirotani, K., & Shibata, S. 2001, ApJ, 558, 216
Kramer, M., et al. 1998, ApJ, 501, 270
Liu, X. F., & Wu, X. J. 1999, Acta Astrophys. Sinica, 19, 68
Luo, Q., Shibata, S., & Melrose, D. B. 2000, MNRAS, 318, 943
Lyne, A. G., & Manchester, R. N. 1988, MNRAS, 234, 477
Romani, R. W. 1996, ApJ, 470, 469
Romani, R. W., & Yadigaroglu, I.-A. 1995, ApJ, 438, 318
Stairs, I. H., Thorsett, S. E., & Camilo, F. 1999, ApJS, 123, 627
Stinebring, D. R., Boriakoff, V., Cordes, J. M., Deich, W. T. S., & Wolszczan, A. 1984, in Birth and Evolution of Neutron Stars: Issues Raised by Millisecond Pulsars, ed. S. P. Reynolds, D. R. Stinebring (Green Bank: NRAO), 32
Sturner, S. J., & Dermer, C. D. 1994, ApJ, 420, L79
Takahashi, M., et al. 2001, ApJ, 554, 316
Thorsett, S. E., & Stinebring, D.R. 1990, ApJ, 361, 644
Xu, R. X. 2002, ApJ, 570, L65
Xu, R. X., Xu, X. B., & Wu X. J. 2001, Chin. Phys. Lett., 18, 837
Zhang, B., & Harding, A. K. 2000, ApJ, 532, 1150